

This is a repository copy of *Virtual HIRF tests in CST STUDIO SUITE™:A Reverberant environment application*.

White Rose Research Online URL for this paper:

<https://eprints.whiterose.ac.uk/132795/>

Version: Accepted Version

---

**Proceedings Paper:**

Tallini, Davide, Dawson, John Frederick [orcid.org/0000-0003-4537-9977](https://orcid.org/0000-0003-4537-9977), Flintoft, Ian David [orcid.org/0000-0003-3153-8447](https://orcid.org/0000-0003-3153-8447) et al. (2 more authors) (2011) Virtual HIRF tests in CST STUDIO SUITE™:A Reverberant environment application. In: ICEAA 2011 International Conference on Electromagnetics in Advanced Applications. , Torino, Italy , pp. 849-852.

<https://doi.org/10.1109/ICEAA.2011.6046454>

---

**Reuse**

Other licence.

**Takedown**

If you consider content in White Rose Research Online to be in breach of UK law, please notify us by emailing [eprints@whiterose.ac.uk](mailto:eprints@whiterose.ac.uk) including the URL of the record and the reason for the withdrawal request.

© 2011 IEEE. Personal use of this material is permitted. Permission from IEEE must be obtained for all other uses, in any current or future media, including reprinting/republishing this material for advertising or promotional purposes, creating new collective works, for resale or redistribution to servers or lists, or reuse of any copyrighted component of this work in other works.

Tallini, D.; Dawson, J.F.; Flintoft, I.D.; Kunze, M.; Munteanu, I., "Virtual HIRF tests in CST STUDIO SUITE™. A reverberant environment application," Electromagnetics in Advanced Applications (ICEAA), 2011 International Conference on , vol., no., pp.849,852, 12-16 Sept. 2011  
doi: [10.1109/ICEAA.2011.6046454](https://doi.org/10.1109/ICEAA.2011.6046454)

keywords: {computational electromagnetics;reverberation;CST STUDIO SUITE;metallic box;reverberant environment application;virtual HIRF test;Aperture antennas;Frequency domain analysis;Probes;Receiving antennas;Time domain analysis},

URL: <http://ieeexplore.ieee.org/stamp/stamp.jsp?tp=&arnumber=6046454&isnumber=6046273>

# Virtual HIRF Tests in CST STUDIO SUITE™

## A Reverberant Environment Application

D. Tallini<sup>1</sup>, J. F. Dawson<sup>2</sup>, I. D. Flintoft<sup>2</sup>, M. Kunze<sup>1</sup>, I. Muntenau<sup>1</sup>

**Abstract** – This paper provides an example of a reverberant environment application. A metallic box in different configurations has been simulated with CST STUDIO SUITE™ and the calculated results have been compared to measurements.

### 1 INTRODUCTION

The prediction of the shielding performances of reverberant environments such as vehicle bodies and metallic enclosure racks is an important part of the global design process of an electromagnetic system in order to ensure predefined performance specifications and fulfill the EMC standards. The desire for a reduced time-to-market means that there is often no time or budget for performing extensive prototyping and test measurements [1]. These limitations make the reliable computation and prediction of the shielding properties of a given structure critical. To speed-up this time-consuming process numerical electromagnetic methods can be successfully adopted to analyze and characterize the system under test in terms of shielding performance.

In this paper the studied test case consists of a metal enclosure, which is illuminated externally, and the internal response observed for different configurations of the internal structure including: coupling to straight and curved single wire lines; coupling through different types of aperture and material in the box walls and loading of the cavity by lossy materials to vary the Q-factor [3].

CST STUDIO SUITE™ has been used to perform the electromagnetic simulations of the previously described configurations.

The results are all presented as a reception aperture, a figure described by the ratio between the power received at a probe antenna and the power density of incident field.

The computed results showed a good agreement with the measured curves over the whole frequency range for all the examined configurations.

In the following, first the description of the analyzed test case set-up (Sec. 2), some comparisons between simulated and measured results are provided (Sec. 3) and some conclusions are drawn (Sec. 4).

### 2 TEST CASE DESCRIPTION

In the next subsections, the test case geometry is described (2.1), the LS22 RAM material (2.2) and then the representative performance observable parameters are illustrated (2.3).

#### 2.1 Metallic box geometry

The validation box is a 600 mm x 500 mm x 300 mm brass box with three removable faces – see Figure 1. Two of the faces (top and side) are permanently closed and the front face is left open or covered with a plate with different characteristics.



Figure 1: Metallic box

In this paper two out of several possible covering plates have been taken into account:

- 1) OF = Open Face
- 2) PP = Perforated Plate

The open face has a 30 mm wide flange around the edge with holes spaced at 26 mm to 28 mm for fixing the covering plate using self-tapping screws.

The perforated plate is a brass plate with a periodic array of circular holes is used for the two-sided impedance boundary measurements. The plate is 0.3 mm thick with 3 mm diameter holes on a regular square grid with spacing 10 mm. The perforation occupies a square of side length 200 mm centered on the front face of the box wall.

The box has three holes for N-type connectors on the top, labeled A, B and C in Figure 3. The probe

<sup>1</sup>CST – Computer Simulation Technology AG, Bad Nauheimer Straße 19, 64289 Darmstadt, Germany.  
e-mail: [davide.tallini@cst.com](mailto:davide.tallini@cst.com), tel.: +49 6151 7303-0, fax: +49 6151 7303-100.

<sup>2</sup> Department of Electronics, University of York, Heslington, York, YO10 5DD, UK.  
e-mail: [jfd@ohm.york.ac.uk](mailto:jfd@ohm.york.ac.uk), tel: +44 1904 322356, fax: +44 1904 323224.

antennas and wire structures are connected to these three ports. Port C is not used in this test case.

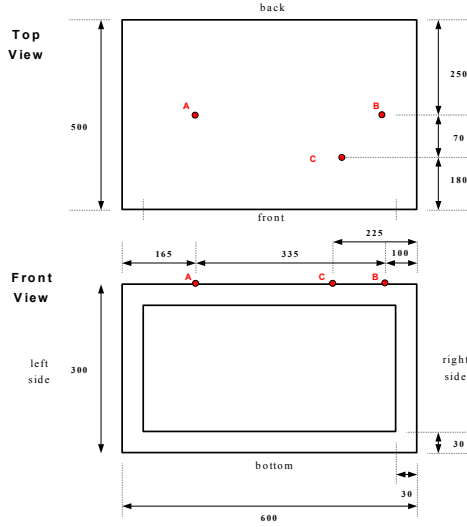


Figure 3 : Sketch views related to the metallic box

Probes with characteristics given in Table 1 are considered – see Figure 4.a). Probes 1 and 2 are nominally identical and they are inserted at ports A and B.

Probe	#1	#2
Length	22 mm	22 mm
Diameter	3 mm	3 mm

Table 1: Probe characteristics

The straight-wire (SW) geometry (see Fig. 4.b) is formed by soldering a horizontal brass rod, 3.5 mm in diameter, between probes 1 and 2 in ports A and B. The curved wire (CW) geometry (see Fig. 4.c) is composed of three semi-circles with two straight extension sections. Ends are soldered into N-Type bulkhead connectors in box ports A and B.

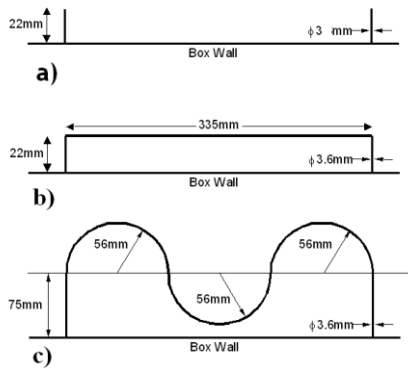


Figure 4: Probe set-up. a) PAPB; b) SW; c) CW

## 2.2 RAM characterization

A cubic piece of Eccosorb LS22 absorber with a side length of 110 mm has been constructed from a number of layers of LS22. The material is characterized by the manufacturer from 500 MHz to 18 GHz via the real and imaginary parts of the complex relative permittivity - see Figure 5:

$$\hat{\epsilon}_r(\omega) = \frac{\epsilon'(\omega) - j\epsilon''(\omega)}{\epsilon_0} \quad (1)$$

It has been placed in different positions inside the box.

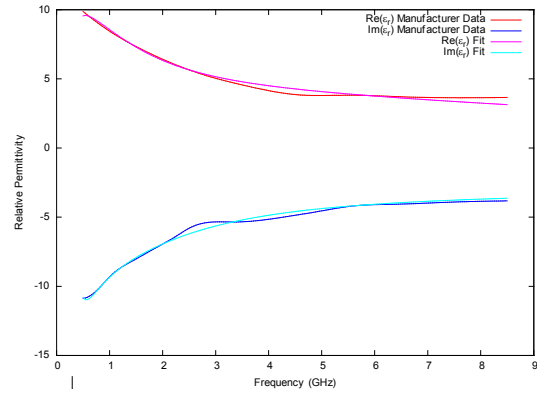


Figure 5: Properties of Eccosorb LS22 (manufacturer's data)

Three cases have been considered:

- 1) A0 – No absorber
- 2) A1 – Absorber in the left corner of the box
- 3) A2 – Absorber in center of the box

## 2.3 Observables

The configurations considered are field-to-probe or field-to-wire couplings. The results are all presented as a reception aperture.

The probe characteristics are presented as an antenna factor (AF), which for an antenna in reception mode is defined by:

$$AF = \frac{E_{inc}}{V_{rec}} \quad (2)$$

$E_{inc}$  = incident electric field strength

$V_{rec}$  = voltage received at the antenna port

The reception aperture and antenna factor are related to the antenna gain by:

$$A_{rec} = \frac{P_{rec}}{S_{inc}} = |S_{21}|^2 \frac{4\pi d^2}{G} = \frac{1}{AF^2} \frac{\eta_0}{Z} \quad (3)$$

$A_{rec}$  - reception aperture ( $m^2$ )

$P_{rec}$  - power received at probe antenna (W)

$S_{inc}$  - power density of incident field ( $W/m^2$ )  
 $d$  – distance from front of box to aperture of horn antenna (1.5 m)  
 $G$  – power gain of horn antenna (-)  
 $AF$  – antenna factor (1/m)  
 $Z$  – impedance of test set ( $\Omega$ )  
 $\eta_0$  - characteristic impedance of free space  
 In decibels reception aperture is related to antenna factor by:

$$A_{rec} (dB / m^2) = 8,77 - AF (dB / m) \quad (4)$$

### 3 SIMULATION RESULTS

#### 3.1 Simulation set-up

CST STUDIO SUITE™ was used to analyze the electromagnetic behavior of the aforementioned configurations. The different geometries have been constructed inside the frontend thanks to its powerful CAD capabilities. A linearly polarized plane wave with amplitude of 1 V/m and hitting orthogonally to the front face has been used as excitation. The receiving probes A and B have been both connected to a matched load (discrete ports with an impedance of 50 Ohm).

The Antenna Factor can be calculated inside CST MICROWAVE STUDIO® by recording the voltage at the discrete port placed in the position A. Taking into account (2) the antenna factor in dB becomes:

$$AF (dB) = 0 - V (dB) \quad (5)$$

Reception Aperture starting from the Antenna Factor can be calculated by means of a simple Template Based Postprocessing.

#### 3.2 Time Domain vs. Frequency Domain

Two different numerical EM methods have been applied to the case-study in order to cross-check the accuracy of the simulated results in the frequency range 1-6 GHz: 1) CST MICROWAVE STUDIO® Transient solver based on the Finite Integration technique (FIT). 2) CST MICROWAVE STUDIO® Frequency Domain solver based on the Finite Element method (FEM).

Since the Transient solver is a broadband method in order to consider the LS22 frequency-dependent material behavior, a general representation consisting of superposition of first and second order model has been applied to fit the RAM complex permittivity data.

The calculated results with both solvers in terms of reception aperture for the case OF-PAPB-A0 have been reported – see Figure 6. A good agreement in terms of reception aperture has been obtained.

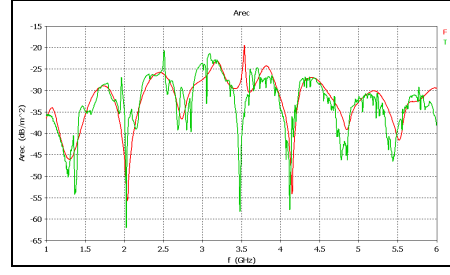


Figure 6: Time Domain vs. Frequency Domain. Reception aperture simulated results (OF-PAPB-A0)

A workstation dual-processor (INTEL XEON 5520) quad-core has been used for the simulations. Some computational effort data related to simulation time and memory requirement have been provided in Table 2.

Method	Time	RAM
FIT	1h 23min	0,37 GB
FEM	6h 26min	13,4 GB

Table 2: Simulation time and memory requirement of OF-PAPB-A0

Since the model is electrically large and the frequency range of interest very wide an algorithm with linear complexity and intrinsically broadband such as the time domain is more efficient than the frequency domain.

The frequency domain curve shows less resonance than the time domain one because the simulation has been performed only on 30 frequency samples.

#### 3.3 Time Domain vs. measured results

The Field-to-Probe Coupling measurement have been performed in a anechoic chamber with a horn antenna illuminating the front place of the box and a Network Analyzer connected to the SMA connectors placed at port A and port B. The measured curves for case OF-PAPB, OF-CWAB have been reported respectively in Figure 7 and Figure 9. The corresponding simulated results have been reported in Figure 8 and Figure 10.

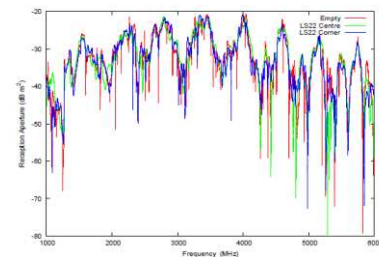


Figure 7: Reception aperture field to probe measurements (OF-PAPB)

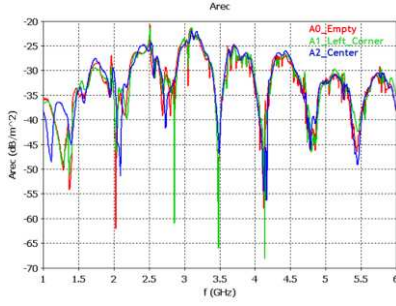


Figure 8: Reception aperture field to probe Time Domain simulations (OF-PAPB)

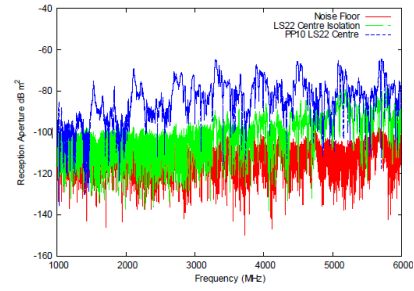


Figure 11: Reception aperture field to probe measurements (blue curve: PP-PPAB-A2)

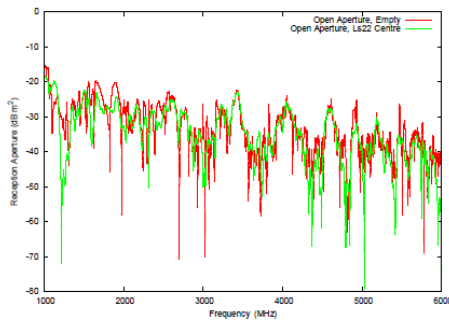


Figure 9: Reception aperture field to curved wire measurements (OF-CWAB)

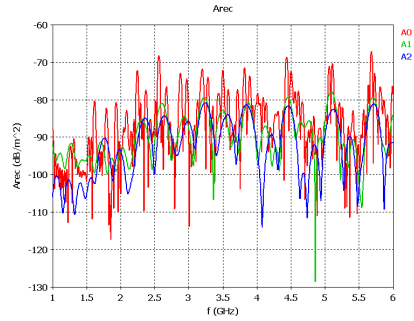


Figure 12: Reception aperture field to probe Time Domain simulations (PP-PPAB)

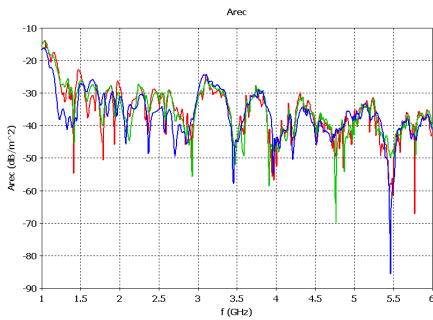


Figure 10: Reception aperture field to curved wire Time Domain simulations (OF-CWAB)

For the perforated plate it has to be noticed that the level of coupling is quite low and very close to the noise level of the measurement system. This type of shielding can be challenging to be simulated due to rapid variation of data over a small frequency range and due to the high sensitivity to small geometric variations in such a strongly resonant environment. Nevertheless the Time Domain simulation was able to capture the right level of coupling as shown in Figure 11 and Figure 12.

## 4 CONCLUSIONS

The analyzed test-case showed the powerfulness of the numerical approach and in particular of the Time Domain solver applied to solve reverberant environment scenario.

## Acknowledgments

The EM simulations have received funding from the EU Seventh Framework Programme (GA/205294, HIRF SE Project) and the measurements from EPSRC (GR/S71552/01, FLAVIIR Project).

## References

- [1] [www.cst.com](http://www.cst.com)
- [2] J. F. Dawson, C. J. Smartt, I. D. Flintoft and C. Christopoulos, "Validating a Numerical Electromagnetic Solver in a Reverberant Environment", IET 7th International Conference on Computation in Electromagnetics, Brighton, 7 April, 2008.
- [3] J. F. Dawson and I. D. Flintoft, "Specification of Numerical Test-case 2 (NTC2): Small 3D Object", Revised Version 1, HIRF SE Consortium, 9th February, 2011.